Journal of Hydroscience and Hydraulic Engineering
Vol. 22, No.1 May, 2004, 25-35

TIME-DEPENDENT STRUCTURE OF HORIZONTAL VORTICES IN UNSTEADY COMPOUND OPEN-CHANNEL FLOWS DURTING RISING AND FALLING STAGES

By

Iehisa Nezu
Professor, Department of Civil Engineering, Kyoto University, Kyoto 606-8501, Japan

Michio Sanjou
Research Associate, Department of Civil Engineering, Kyoto University, Kyoto 606-8501, Japan

and

Ken Goto
Graduate Student, Department of Civil Engineering, Kyoto University, Kyoto 606-8501, Japan

SYNOPSIS

Compound open-channel flows are often observed in actual rivers. They are two-stage flows composed of a main-channel and floodplains. At the junction region between the main-channel and floodplain, a coherent horizontal vortex appears, and it has a significant influence on flow structure and the associated water environment. Therefore, many experimental and numerical researches have been conducted on such horizontal vortices. However, most of them have been studied on the depth-fixed steady compound open-channel flows, and there is no database of the time-dependent properties of horizontal vortices in depth-varying and channel-changing compound free-surface flows, i.e., during the rising and falling stages of floods. Therefore, in the present study, PIV measurements were conducted in the time-dependent and depth-varying unsteady compound open-channel flows, and the generation and development processes of horizontal vortices were investigated in detail. It was shown experimentally that the spanwise profiles of primary velocity have a significant effect on the time-dependent horizontal eddy structure.

INTRODUCTION

There are some large-scale horizontal vortices with a vertical axis in compound open-channel flows. It is very important to examine such vortex structures because these horizontal vortices influence significantly the transverse transport of scalar variables such as suspended sediment between the main-channel and floodplains. Sellin (1966) found by using the powder of aluminum that some horizontal vortices exist in the streamwise direction with a constant spacing. Tamai *et al.*(1986) investigated experimentally a generation process of periodical horizontal eddies by using a flow-visualization technique. Ikeda *et al.*(1992) have studied the horizontal vortices in terms of instability analysis in symmetric compound open-channel flows. Ishigaki & Imamoto(1995) have investigated experimentally a

Table 1 Hydraulic condition

case	H_b (cm)	H_p (cm)	B_f/B	H_b/D	H_p/D	Q_b (l/s)	Q_p (l/s)	Um_b (cm/s)	Um_p (cm/s)	T_d (s)	α ($\times 10^{-3}$)
HH60	7.5	10.5	0.5	1.5	2.1	2.1	14.4	10.5	45.0	60	1.8
TH60	4.0	8.3	0.5	0.8	1.7	2.3	13.8	28.8	59.4	60	1.6

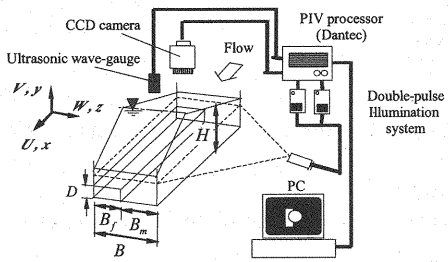

Fig.1 Experimental flume and PIV system

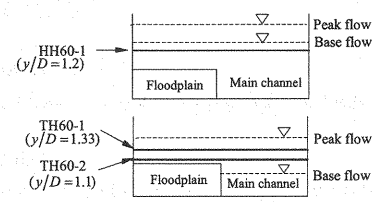

Fig.2 Elevation of laser light sheet

relation between horizontal vortices and secondary currents in a compound open-channels. Nezu & Nakayama(1997) showed the space-time structures of horizontal eddies in compound open-channel flows by PTV (particle tracking velocimetry) measurements. Nezu *et al.*(1999) have conducted some turbulence measurements in shallow and deep floodplain compound open-channel flows by using both LDA(laser Doppler anemometer) and PIV(particle image velocimetry). They found that a single-vortex line was generated between the floodplain and main-channel for shallow floodplain-depth, whereas a twin-vortex line was generated for deep floodplain-depth. Recently, with the development of computer system and turbulence modeling, numerical studies have also been conducted intensively. For example, Nadaoka & Yagi(1998) and Bousmar & Zech(2001) have simulated the compound open-channel flows by using a depth-averaged LES model and predicted a coherent structure of horizontal vortices.

However, unsteadiness properties of horizontal vortices in depth-varying rectangular/compound open-channel flows with channel-changing process have not yet been revealed. Therefore, in this study, turbulence measurements were conducted in the time-dependent and depth-varying unsteady compound open-channel flows using a YAG-laser PIV system and, consequently, the generation and development mechanism of horizontal vortices were investigated in detail.

EXPERIMENTAL PROCEDURE AND HYDRAULIC CONDITIONS

Fig.1 shows the experimental setup used in this study. The experiments for this study were conducted in a 10m long, 40cm wide and 30cm deep tilting flume. The 5cm height acrylic boxes were set on the right hand side of the channel flume as a floodplain. In this figure, B is the channel width, B_f is the floodplain width, B_m is the main-channel width, H is the water depth, and D is the height of floodplain. In the present experiments, $D=5$ cm and $B_f/B=1/2$ were chosen. Coordinates x, y and z denotes the streamwise, vertical and spanwise directions, respectively. U , V and W are the ensemble-averaged velocity components in each direction. u , v and w are the turbulent components. The time-dependent discharge $Q(t)$ can be controlled automatically by a computer system involved with electromagnetic flow-meter. The discharge hydrograph was given here by a triangular wave.

The turbulence measurements were conducted by the PIV system (DANTEC). The seeding particles, which have a diameter of 100 μ m and are made of Nylon 12(specific gravity is 1.01), were uniformly scattered in the recirculating water of the flume. A 15(mJ) Yag double-pulse laser beam was used to illuminate the flow field as a 2mm thick laser light sheet (LLS). A pair of images (200mm×200mm) of tracers were taken by making use of a high-sensitive CCD camera(1008 pixel×1008 pixel, KODAK) which was placed above the free surface. The time-dependent water depth was measured by an ultrasonic wave gauge. In the present study, free-surface fluctuation of the peak depth was almost same as that of the base depth, and thus, PIV accuracy did not change remarkably during flood stages.

In this study, two kinds of depth-varying unsteady compound open-channel flows were treated. Table1 shows these hydraulic conditions, in which Um is the mean bulk velocity, i.e., $Um = Q/A$. T_d is the duration time from the base-flow depth to the peak-flow one. The subscripts b and p denote the base and peak flows, respectively. α is an unsteadiness parameter proposed by Nezu & Nakagawa(1993), and it is given by

$$\alpha \equiv \frac{1}{(U_{mb}+U_{mp})/2}\cdot\frac{H_p - H_b}{T_d} \qquad (1).$$

The unsteadiness of the present measurements is about one hundred times as large as that of actual rivers in flood.

Case HH is the depth-varying open-channel flow from a compound to compound channels. The other case TH is the unsteady free-surface flow with the transition process from a rectangular to compound channels. These cases were selected as including the transitional-depth of $H/D = 1.5$ between the single eddy structure and twin eddy structure pointed out by Nezu *et al.*(1999).

Fig.2 shows the elevations of the laser light sheet(LLS) projected into the flume water. Three PIV measurements indicated in Fig.2 are referred here to HH60-1 ($y/D = 1.2$), TH60-1 ($y/D = 1.33$) and TH60-2 ($y/D = 1.1$), respectively.

RESULTS AND DISCUSSION

Time-variation of water depth and primary velocity

Fig.3 shows the time-dependent water depth $H(t)$ in the main-channel measured by an ultrasonic wave gauge. From this result, the water depth H increases and decreases with time t in both cases. The depth-varying unsteady stage can be classified by the normalized time $T \equiv t/T_d$. That is to say, $T \equiv 1$ is the peak-depth time, and $0 < T < 1$ and $1 < T < 2$ are the rising and falling stages, respectively.

Fig.4 shows the time-variations of normalized primary velocity $U(T)$ in the case of HH60-1, in which $\overline{U}_b$ is the spanwise-averaged primary velocity at $T = 0.0$ (base). From these results, it is found that the time-variations of U are larger in the rising stage than in the falling stage. It is of significant importance that the floodplain velocity at $z/B = -0.2$ becomes larger than the junction velocity at $z/B = 0.0$ with an increase of the water depth. This fact implies that the velocity structure may vary remarkably with time as will be mentioned later. Furthermore, it should be noticed that the peak values appear before the peak depth time ($T = 1.0$). This means that the relation between velocity and water depth is not symmetrical in the rising and falling stages. In particular, from Fig.3 and Fig.4, the

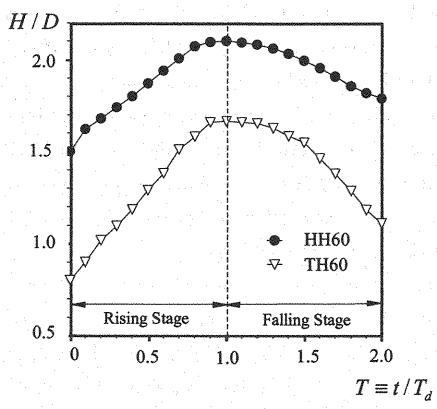

Fig.3 Time-variations of water depth

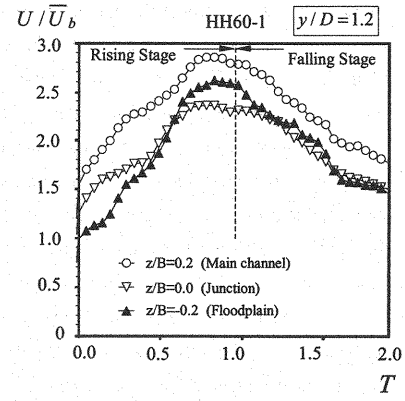

Fig.4 Time-variations of primary velocity

time-variation in the rising stage is larger than that in the falling one for both primary velocity U and water depth H .

Instantaneous velocity vectors

Fig.5 shows the distributions of instantaneous velocities($\hat{u}$, $\hat{w}$) and the corresponding vorticity ω_y in the case of HH60-1(compound to compound). The instantaneous velocity vectors $\hat{u}$ and $\hat{w}$ are described in the movable coordinate, where the space-averaged velocities U_{mean} and W_{mean} are subtracted from the original instantaneous velocities $\tilde{u}$ and $\tilde{w}$, i.e., $\hat{u} \equiv \tilde{u} - U_{mean}$ and $\hat{w} \equiv \tilde{w} - W_{mean}$. The vorticity component ω_y is defined as follows:

$$\omega_y \equiv \frac{\partial \hat{u}}{\partial z} - \frac{\partial \hat{w}}{\partial x} = \frac{\partial (\tilde{u} - U_{mean})}{\partial z} - \frac{\partial (\tilde{w} - W_{mean})}{\partial x} \qquad (2)$$

In Fig.5, x means the vortex-core positions estimated approximately from the distributions of instantaneous velocity vectors and the corresponding vorticity.

At the base-flow stage $T = 0.0$ and the rising stage $T = 0.5$, there is a clockwise single eddy near the junction between the main-channel and floodplain. On the other hand, at the peak-depth stage $T = 1.0$, twin eddies which rotate in the opposite directions are observed, and the distributions of vorticity ω_y have positive value in the main-channel and negative one on the floodplain. At the falling stage $T = 1.5$, the main-channel eddy is even now observed, whereas the floodplain eddy is disappearing. At the base back discharge stage $T = 2.0$, the floodplain eddy almost disappears and only a single horizontal vortex is observed near the junction as seen for the shallow floodplain stages of $T = 0.0$ and $T = 0.5$.

Fig.6 shows the streamwise distributions of instantaneous spanwise velocity $\tilde{w}(t)$ in the eddy-existing region for HH60-1, i.e., the junction of $z = 0$ at $T = 0.0$, the main-channel of $z = 0.1$ and the floodplain of $z = -0.1$ at $T = 1.0$. The results are indicated at three time phases with a short time span of 0.33 seconds. We can see the periodical distributions of spanwise velocity, and it can be recognized from Fig.6 that coherent horizontal eddies are transported downstream.

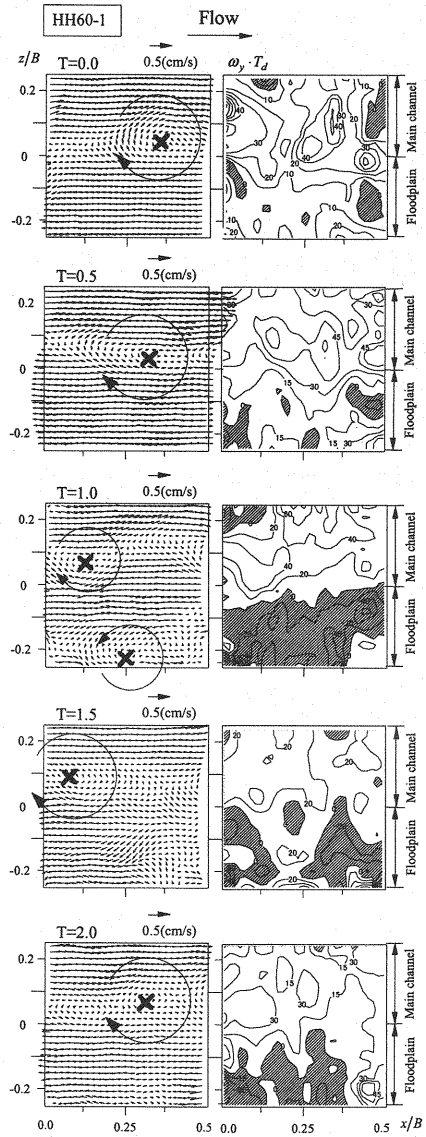

Fig. 5 Instantaneous velocity vectors for case HH60-1 (x means core position)

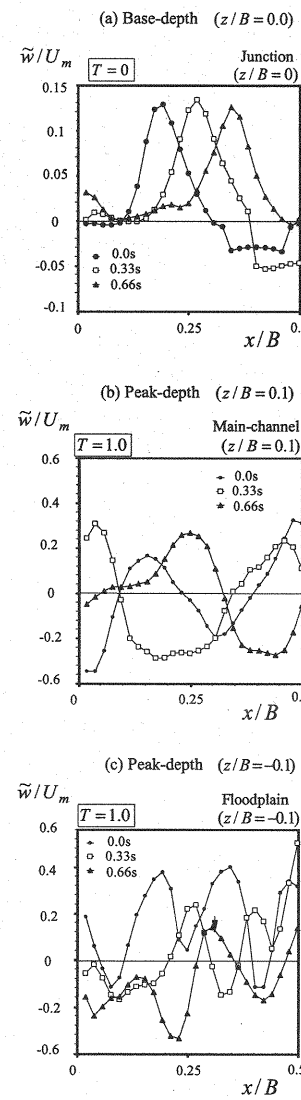

Fig.6 Streamwise distributions of spanwise velocity component

Fig.7(a) shows the instantaneous velocity vectors in the channel-changing flow case (from rectangular to compound) of TH60-1 at $y/D = 1.33$, in which the elevation of LLS was near the free-surface. At the shallow floodplain stage of $T = 0.5$, an inundation flow toward the floodplain is observed, and a single eddy appears at the junction in the same manner as all compound-channel cases of HH60-1. However, since the flow turbulence due to cross sectional transition from the rectangular to compound channels becomes strong, the coherent structures are not observed so clearly as HH60. At

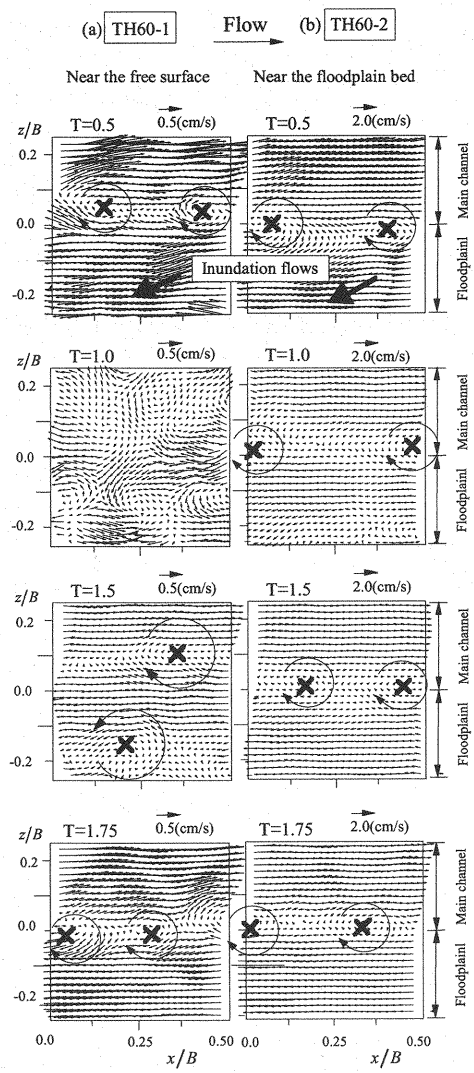

Fig.7 Instantaneous velocity vectors for case TH60-1 (channel-changing case from rectangular to compound)

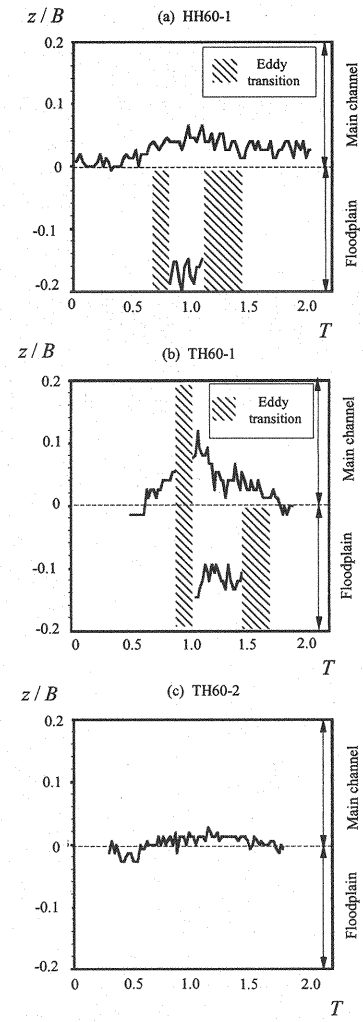

Fig.8 Time-variations of vortex core-position

peak-depth stage $T = 1.0$, a developing eddy is observed in the floodplain zone. At the falling-depth stage $T = 1.5$, twin horizontal eddies are observed on both the main-channel and floodplain. At the shallow floodplain stage $T = 1.75$, the structure of horizontal vortex returns to single one.

Fig.7(b) shows the distributions of instantaneous velocities in the case TH60-2 at $y/D = 1.1$, in which the measuring plain was set near the floodplain bed. At $T = 0.5$, there is a single horizontal eddy at the center of the channel in the same manner as TH60-1 ($y/D = 1.33$). However, it should be pointed out that the single eddy is still observed near the junction of floodplain at $T = 1.0$. Contrary to HH60-1 and TH60-1, the floodplain eddy cannot be observed. At the falling-depth stages $T = 1.5$ and $T = 1.75$, a single

horizontal vortex is observed. From these interesting results, it is found that the structure of horizontal eddy near the floodplain bed does not change into the twin-eddy structure even in all depth-varying stages.

Time-dependent property of vortex-core position

Fig.8 shows the time-variations of vortex-core position in the spanwise direction of the horizontal eddies. In the case of HH60-1and TH60-1, a single eddy exists near the junction in the shallow depth stages($0 < T < 0.5$). As the water depth increases, this horizontal eddy moves toward the main-channel region. At the same time, another eddy appears in the floodplain region. At the falling stage ($1.5 < T < 2.0$), the coherent eddy has a single structure again. On the other hand, in the TH60-2 which is near the floodplain bed, the single-eddy structure is observed even in the deep depth stage. The reason for this is that there is a difference of primary velocities between the main-channel and floodplain in all the time stages and thus an inflectional instability of flow is generated near the junction, which will be discussed in the following section.

Spanwise profiles of primary velocity

Fig.9 shows the spanwise profiles of the primary velocity $U(z)$ as a function of time T . In the case of HH60-1, the values of U are normalized by the spanwise-averaged velocity $\overline{U}_b$ at the base-flow time ($T = 0.0$). At the shallow-stage time of $T = 0.0$ and $T = 0.5$, there are significant differences in the primary velocity between the main-channel and floodplain, that is to say, the primary velocity is much larger in the main-channel than in the floodplain region. What is of particular significance is that the distributions of $U(z)$ in the shallow water stage have only a single inflectional point, which is the cause of shear instability near the junction. This feature was pointed out by Ikeda *et al.*(1992). At $T = 1.0$, the distribution of $U(z)$ decreases locally near the junction due to secondary currents that transport the low-speed fluids from the junction edge toward the free surface, and consequently two inflectional points are observed. This fact strongly suggests a generation of twin horizontal eddies with counter-rotating vortex, as pointed out by Nezu *et al.*(1999).

In the cases of TH60-1 and TH60-2, the values of $U(z)$ are normalized by the spanwise-averaged velocity $\overline{U}_{50}$ at $T = 0.5$. The velocity distributions of TH60-1 show similar pattern as those of HH60-1. Two inflectional points are observed at the peak-depth time $T = 1.0$. In contrast, in the case of TH60-2 in which the LLS elevation is near the floodplain bed, there is only a single inflectional point near the junction in all compound-channel stages. This fact may be due to the floodplain wall shear stress prevents an increase of primary velocity near the floodplain bed even at $T = 1.0$. As for the results, in the case of TH60-2, which is the near-wall measurement, only a single vortex structure is generated even though the flow depth increases, as seen in Fig.7(b). From these facts it is strongly inferred that the structure of horizontal eddies is largely dominated by such an inflectional instability.

Ikeda *et al.*(1997) conducted an instability analysis and revealed that the velocity shear in the spanwise direction generates the horizontal vortex. From their findings and the present experimental results, it is thought that the velocity distribution along the perimeter has strong effects on the time-dependent development process of horizontal eddies. Therefore, the following shear parameter γ was proposed to estimate a time-dependent vortex structure in this study.

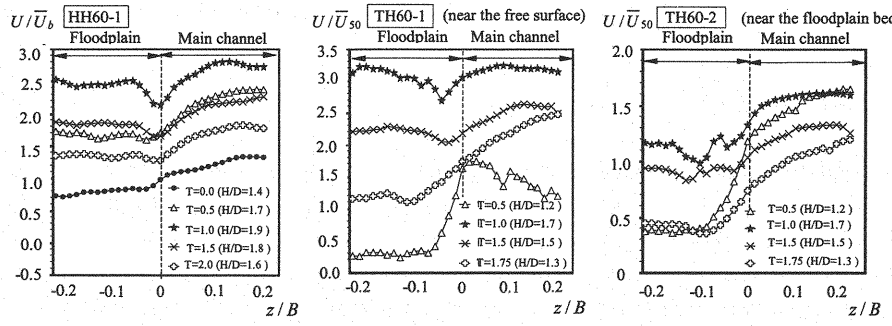

Fig.9 Spanwise profiles of primary velocity

$$\gamma = \frac{\widetilde{u}_m - \widetilde{u}_j}{\widetilde{u}_m - \widetilde{u}_f} = \frac{\widetilde{u}_j - \widetilde{u}_m}{\widetilde{u}_f - \widetilde{u}_m} \qquad (3)$$

in which, $\widetilde{u}_m$, $\widetilde{u}_j$ and $\widetilde{u}_f$ are the instantaneous primary velocities at the main-channel $(z/B = 0.2)$, junction $(z/B = 0)$ and floodplain $(z/B = -0.2)$, respectively. In the case of $\gamma < 1$, the primary velocity decreases monotonically from the main-channel to floodplain, that is to say, there is a single inflectional point near the junction between the main-channel and floodplain. On the other hand, in the case of $\gamma \geq 1$, the velocity distribution decreases locally near the junction; there is a possibility of two inflectional points. It is considered that as the value of γ becomes larger, such a local velocity-dip property becomes more remarkable and consequently twin eddies may be more frequently generated. Fig.10 shows the time-variations of γ. The duration time of twin- eddy stage is also indicated in this figure. From Fig.10, it is judged that the time-range of $\gamma > 2$ coincides well with that of twin-eddy structure observed in HH60-1 and TH60-1. On the other hand, γ is certainly smaller than 1 in all time-stages for the near-bed case of TH60-2.

Time-dependent distributions of spanwise Reynolds stress

Fig.11 shows a relation between the instantaneous streamwise and spanwise velocity components, $\hat{u}$ and $\hat{w}$ during a constant time span for HH60-1. The spanwise test position z/B and corresponding time-stage T are as same as shown in Fig.6, i.e., the eddy-existing region. From these results, a correlation between the two components corresponds to the rotating directions of horizontal eddies indicated in Fig.5.

Fig.12 shows the time-dependent distributions of spanwise Reynolds stress $-\overline{uw}$ against the perimeter z/B. These values are

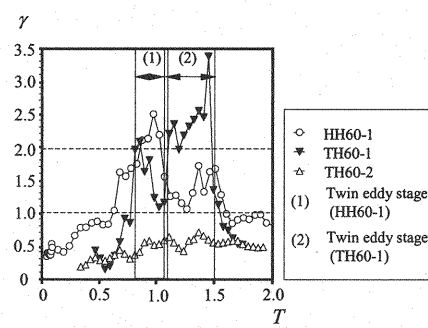

Fig.10 Time-variations of shear parameter λ

normalized by the spanwise-averaged velocity $\overline{U}_b$. At the shallow-stage time of $T = 0.0$, there is a maximum positive value in the junction region. This fact reveals that the coherent vortices promote the mass and momentum transport between the main-channel and floodplain. On the other hand, at the deep- stage time of $T = 1.0$, the value of $-\overline{uw}$ takes the positive one near the junction in the main-channel region, whereas it takes the negative one near the junction in the floodplain region. From these results and Fig.5, it is inferred that these features have strong correlations with the above-mentioned structures of horizontal eddies.

Time-dependent structure model of horizontal vortices

Fig.13 shows the schematized hydrodynamic model of the horizontal vortices in unsteady depth-varying compound open-channel flows. In the shallow base-flow stage, there are remarkable differences in primary velocities between the main-channel and floodplain, and consequently only a single horizontal eddy is generated by a shear instability of primary velocity. What is of particular significance is that horizontal vortices are transported from the junction toward the floodplain region by inundation flows. This phenomenon is peculiar to the channel-changing and depth-varying unsteady flows and it is not observed in depth-fixed steady flows. With an increase of floodplain depth, the spanwise distribution of primary velocity decreases locally at the junction due to secondary flow near the free-surface, and consequently, another vortex appears on the floodplain and the counter-rotating twin horizontal eddies are observed in the deep rising stage. On the other hand, a single eddy structure is observed near the floodplain bed even in the peak stage because velocity profile has a similar pattern to that of base stage. In the falling stage, floodplain vortex disappears with a decrease of water depth, and the main-channel vortex moves back to the junction of compound channel again.

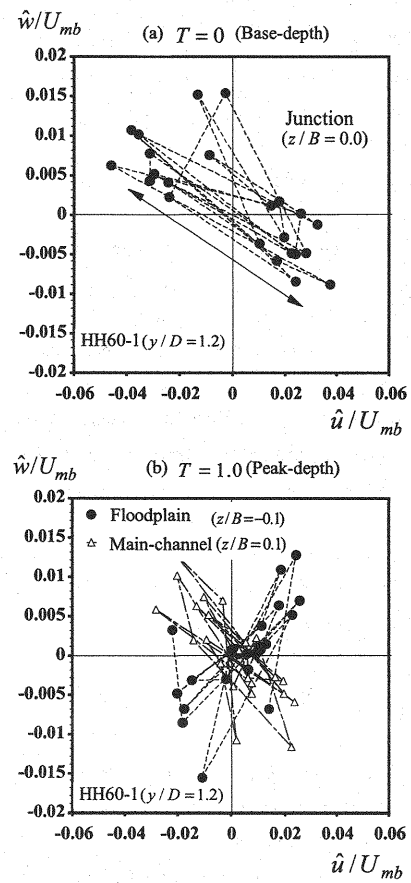

Fig.11 Relation between the instantaneous streamwise and spanwise velocity components

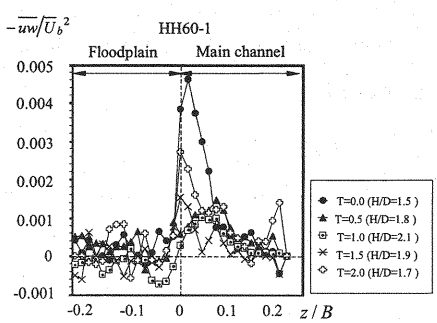

Fig.12 Spanwise profiles of Reynolds stress

CONCLUSIONS

The birth and developing mechanism of coherent horizontal vortices in depth-varying unsteady open-channel flows were investigated experimentally. The main findings of this study are as follows:

1) In depth-varying unsteady open-channel flows, a single horizontal eddy appears near the junction region in the shallow-water stage. On the other hand, another vortex is generated on the floodplain in the deep-water stage, and consequently twin-eddies structure is observed clearly.

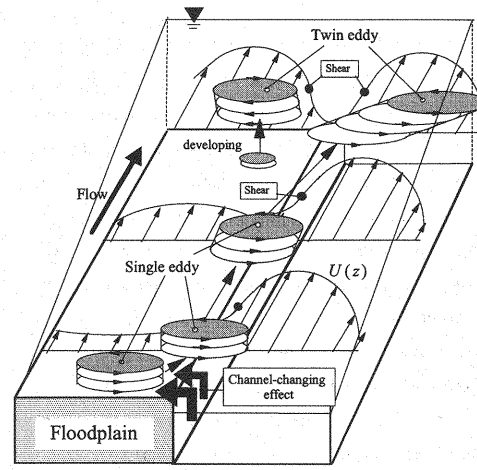

Fig.13 Schematized model of horizontal eddies in depth-varying unsteady compound open-channel flow

2) The structure of a horizontal eddy is largely dominated by the spanwise profiles of primary velocity. In the base-flow stage, there is only one inflectional point in the distribution of primary of velocity. In contrast, at the peak-flow time, there are two inflectional points due to the local decrease, i.e., velocity-dip phenomena near the junction. Such a time-dependent property of velocity has a significant influence on horizontal vortices.

3) At the base flow, the spanwise Reynolds stress $-\overline{uw}$ takes a maximum value near the junction, and it is inferred that a single horizontal eddy promotes the transverse momentum and mass transport. In contrast, at the peak flow, the value of $-\overline{uw}$ takes a positive value in the main-channel region and negative one in the floodplain region. From these properties, it is found that such time-dependent structure of Reynolds stress has a strong correlation with that of horizontal eddy.

REFERENCES

1. Bousmar, D. and Zech, Y.: Periodic turbulent structures modeling in a symmetric compound channel, *Proc. of 29th Corgress,* Beijin, Theme D, pp.244-249, 2001.
2. Ikeda, S., Ohta, K. and Hasegawa, H.: Periodic vortices at the boundary of vegetated area along river bank, *J. of Hydraulic, Coastal and Envir. Eng.*, JSCE, No.443/II-18, pp.47-54, 1992.(in Japanese).
3. Ishigaki, T. and Imamoto, H.: Experimental study on 3-D flow structure in compound open channel, *J. of Hydraulic Coastal and Envir. Eng.*, JSCE, No.515/II-31, pp.45-54, 1995.(in Japanese).
4. Ikeda, S. and Kuga, T.: Laboratory study on large horizontal vortices in compound open channel flow, *J. of Hydraulic, Coastal and Envir. Eng.*, JSCE, No.558/II-38, pp.91-102, 1997.(in Japanese).
5. Nadaoka, K. and Yagi, H.: Shallow-water turbulence modeling and horizontal large eddy

computation of river flow, *J. of Hydraulic Eng.*, ASCE, vol.124, No.5, pp.493-500, 1998.

6. Nezu, I. and Nakagawa, H.: Basic structure of turbulence in unsteady open channel flows, *Proc. of 9th Int. Symposium on Turbulent Shear Flows*, Kyoto, pp.7.1.1-7.1.6., 1993.
7. Nezu, I. and Nakayama, T.: Space-time correlation structures of horizontal coherent vortices in compound open-channel flows by using particle-tracking velocimetry, *J. of Hydraulic Research*, IAHR, vol.35, No.2, pp.191-208, 1997.
8. Nezu, I., Kadota, A. and Nakagawa, H.: Turbulent structure in unsteady depth-varying open-channel Flows, *J. of Hydraulic Eng.*, ASCE, Vol. 123, pp.752-763, 1997.
9. Nezu, I. Onitsuka, K., and Iketani K.: Coherent horizontal vortices in compound open-channel flows, *HYDRAULIC MODELING*(ed. Singh et al.), Water Resources Pub., Colorado, pp.17-32, 1999.
10. Sellin, R.H.J.: A laboratory investigation into the flow in the channel of a river and that over flood plain, *La Houille Blanche*, No.7, pp.22-26, 1964.
11. Tamai, N., Asaeda, T. & Ikeda, H.: Study on generation of periodical large surface eddies, *Water Resources Research*, vol.22, No.7, pp.1129-1138, 1986.

APPENDIX – NOTATION

The following symbols are used in this paper:

A	=	flowing area;
B	=	channel width;
B_m	=	main-channel width;
B_f	=	floodplain width;
D	=	floodplain height;
H	=	water depth in the main-channel;
$T \equiv t / T_d$	=	normalized time;
T_d	=	duration time between base and peak depth;
Q	=	water discharge;
U, V, W	=	mean velocity components;
u, v, w	=	turbulence components;
Um	=	bulk-mean velocity
ω_y	=	vorticity component in the vertical axis y ;
λ	=	shear parameter defined by (3)
b, p	=	subscripts for base and peak flows.

(Received June 12, 2003 ; revised October 8, 2003)